PAPER *Special Section/Issue on ******

Shot Noise Modeling in Metal-Oxide-Semiconductor Field Effect Transistors under Sub-Threshold Condition

Yoshioki Isobe[†], Kiyohito Hara, Dondee Navarro[††], Youichi Takeda[††], Tatsuya Ezaki[††] and Mitiko Miura-Mattausch[††]

Summary
We have developed a new simulation methodology for predicting shot noise intensity in Metal-Oxide-Semiconductor Field Effect Transistor (MOSFET). In our approach, shot noise in MOSFETs is calculated by employing the two dimensional device simulator MEDICI in conjunction with the shot noise model of p-n junction. The accuracy of the noise model has been demonstrated by comparing simulation results with measured noise data of p-n diodes.
The intensity of shot noise in various n-MOSFET devices under various bias conditions was estimated beyond GHz operational frequency by using our simulation scheme. At DC or low-frequency region, sub-threshold current dominates the intensity of shot noise. Therefore, shot noise is independent on frequency in this region and its intensity is exponentially depends on V_G, proportional to L^{-1}, and almost independent on V_D. At high-frequency region above GHz frequency, on the other hand, shot noise intensity is frequency dependent and is quite larger than that of low-frequency region. In particular, the intensity of the RF shot noise is almost independent on L, V_D and V_G. This suggests that high-frequency shot noise intensity is decided only by the conditions of source-bulk junction.

Key words:
mosfet, shot noise, high frequency noise, simulation, sub-threshold current

1. Introduction

In future device engineering, the switching speed becomes higher and the power of signal becomes smaller. To improve device performances, minimization of semiconductor devices is one of the key technologies to derive smaller signal on higher frequency. Recently, with decreasing device size and its driving power, the noise amplitude tends to be enhanced and signal/noise ratio becomes worse. This causes malfunction of analog devices or deterioration of switching performance of digital devices. Therefore, micro device design must be based on understanding of noise generation mechanism to achieve intentional performance.
Among noise sources in Metal-Oxide-Semiconductor Field Effect Transistors (MOSFETs), 1/*f* and thermal noise are dominant at low frequency and have been studied in detail experimentally and theoretically [1-16]. These noises are generated at channel region in MOSFET. At higher frequency region, on the other hand, additional noise sources become observable especially in short-channel devices. In the case of thin-oxide MOSFET, gate capacitance and gate leak current become large. This causes gate induced noise and gate current shot noise respectively [17-22]. In short-channel MOSFET, the effect of junction between substrate and doped region becomes dominant relative to channel region. As a result, noise generated in the junction rises instead of channel thermal noise. This new junction noise should be shot noise.
The shot noise is generated when current flows across potential barrier [1-2]. Figure 1 shows the cross section of n-MOSFET with two possible sources of shot noise. In the past papers for MOSFET, such shot noise is considered to be quite smaller than channel thermal noise and ignorable [12, 23]. From recent works, however, gate leak current I_G through gate oxide of thickness t_{OX} causes enhancement of shot noise when t_{OX} < 2nm under sufficient gate voltage V_G [18, 22]. The other source of shot noise is drain current I_D at p-n junction potential barrier. Obrecht *et al*. calculated that the shot noise become dominant at short channel length L about $L \sim 0.5\mu m$ [24-25].

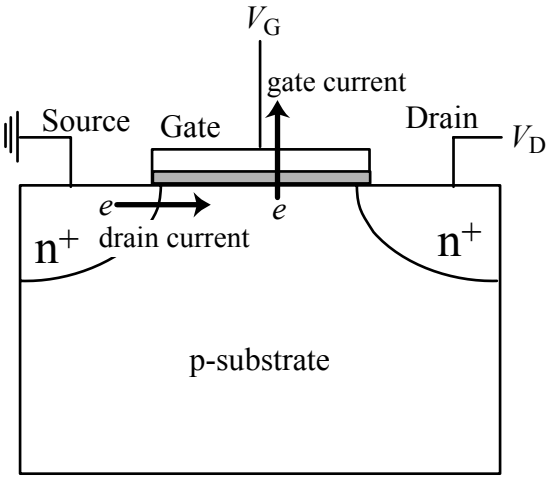

Fig. 1 Two major shot noise sources in n-MOSFET. The arrows indicate electron flow that generates shot noise.

Manuscript received ##########.
Manuscript revised ##########.
[†] The author is with Hiroshima University, Higashihiroshima, 739-8530,

In this paper, we extend the shot noise model of p-n diode to drain current of n-MOSFET in weak inversion. The measurement system for device current noise spectrum density is explained in section 2. In section 3, we introduce shot noise model equation of p-n diode and extend this model to n-MOSFET. The validity of the model of p-n diode is confirmed by comparing to noise measurement at the top of section 4. In the rest of section 4, we perform calculation of shot noise spectrum intensity for n-MOSFET by 2-D device simulator MEDICI, and discuss about its bias, channel length, or frequency dependency.

2. Measurement

In this paper, the purpose of measurement is to compare with theoretical shot noise spectrum and confirm the validity of shot noise model. The measurement system and circuit for noise spectrum intensity are shown in Fig. 2. Semiconductor parameter analyzer HP4156 is used for DC source and vector signal analyzer HP89410 is used to analyze output signal. As shown in Fig. 2, input DC bias V_{in} is applied to device under test (DUT) through noise-cut filter to exclude external noises. We use p-n diode as DUT because shot noise is evidently observed.

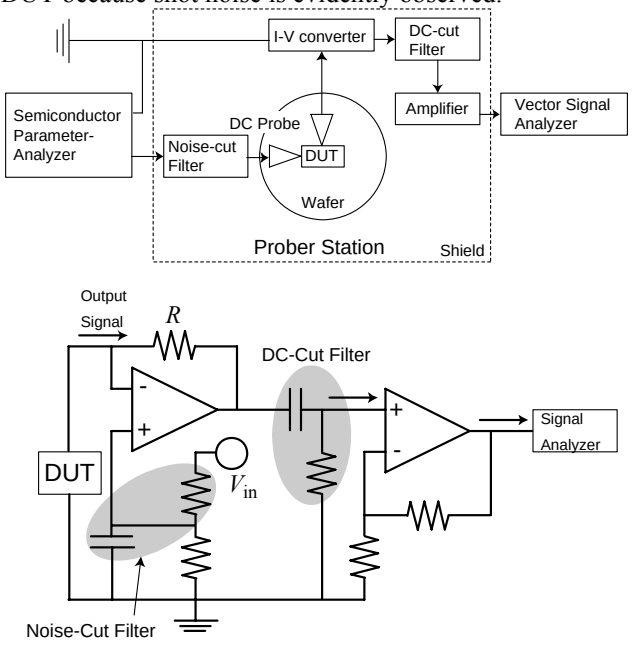

Fig. 2 Measurement system and circuit for our noise spectrum observation. DUT for shot noise measurement is p-n diode because MOSFET shot noise is quite small.

The output current signal $I + \Delta I$ which including current fluctuation ΔI satisfies the relation

$$I = gV_{in}, \tag{1}$$

$$\Delta I = g\Delta V, \tag{2}$$

where g is conductance and ΔV is voltage fluctuation in DUT. Then I-V converter with resistance R and DC-cut filter extract voltage fluctuation component ΔV_{out} from output signal as

$$\Delta V_{out} = -R\Delta I = -Rg\Delta V. \tag{3}$$

Then output signal is amplified by gain A. Thus measured voltage fluctuation ΔV_{meas} is

$$\Delta V_{meas} = A\Delta V_{out} = -AR\Delta I. \tag{4}$$

The relation between measured voltage noise spectrum $S_{V,meas}(f)$ and measured fluctuation ΔV_{meas}, and device current noise spectrum $S_I(f)$ and the fluctuation ΔI, are as follows:

$$S_{V,meas}(f) = \frac{\overline{\Delta V_{meas}^2}}{\Delta f}, \tag{5}$$

$$S_I(f) = \frac{\overline{\Delta I^2}}{\Delta f}. \tag{6}$$

Therefore, voltage spectrum density $S_{V,meas}(f)$ observed on signal analyzer is transferred to current spectrum density $S_I(f)$ of the device as

$$S_I(f) = \frac{S_{V,meas}(f)}{A^2R^2}. \tag{7}$$

For the purpose of system noise reduction, the measurement system and circuit should avoid ground loop and noisy device. In the design of measurement circuit, we use OP amp of bipolar device which is less noisy than MOS device. The frequency measurement limit of our circuit, which is determined by cut-off frequency of OP amp, is about 1MHz. Additionally, low-dielectric material is used for circuit substrate to reduce parasitic capacitance. The measurement limit of noise amplitude, mainly determined by parasitic capacitance of measurement circuit, is about 10^{-23} A^2/Hz.

3. Shot Noise Model for MOSFET

As shown in Fig. 1, shot noise in MOSFET is generated by drain current across junction potential barrier and by gate leak current across gate oxide. Now we focus on drain current shot noise and ignore gate current. In this sight, n-MOSFET is assumed to two p-n junctions sharing p region as channel region.

3.1 Shot Noise in p-n Junction

In general, shot noise originates the discrete flow of carriers across potential barrier. The current shot noise spectral density is given by [19-20]

$$S_I(f) = 2qI, \tag{8}$$

where q is electron charge and I is current which flows across the potential barrier.

In the case of ideal p-n junction, the height of junction potential barrier under zero bias is defined as built-in potential. This barrier height is increased by reverse bias and decreased by forward bias. Under forward bias larger than built-in potential, the barrier is diminished and shot noise is no longer generated. Thus we consider bias condition less than built-in potential. Conduction current I of p-n junction under forward bias V is described by Shockley equation as

$$I = I_0\left(e^{qV/kT} - 1\right), \tag{9}$$

$$I_0 = S\left(\frac{qD_n n_{p0}}{L_n} + \frac{qD_p p_{n0}}{L_p}\right), \tag{10}$$

where k is Boltzman constant, T is absolute temperature, and S is cross section of the junction. n_{p0} and p_{n0} are equilibrium density of electron in p region and hole in n region, respectively. $L_{n,p}$ is diffusion length of electron or hole and $D_{n,p}$ is diffusion coefficient of electron or hole. Here, I_0 is called as junction saturation current. From Eq. 9, DC current I in p-n junction is made of two components, $I_0 \exp(qV/kT)$ and $-I_0$. Additionally, I_0 is quite small and $I >> I_0$ at $V > kT/q \sim 0.03$V.

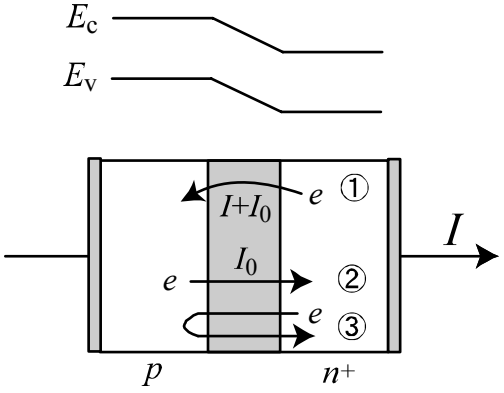

Fig. 3 The energy band shape in p-n$^+$ junction and three electron flow components in p-n$^+$ diode; (1) electrons drifting from n$^+$ to p region across potential barrier, (2) electrons flowing from p to n$^+$ region along potential decay, and (3) electrons drifted from n$^+$ and returned to n+ region by back diffusion. The gray region is depletion layer including junction potential barrier.

Van der Ziel reported that shot noise in p-n$^+$ diode is generated when electron crosses junction potential barrier because almost all current is carried by electron [2]. Here, the electron flow is consists of three components as shown in Fig. 3: 1) Electrons drifted from n$^+$ to p region and then recombine with holes or reach to electrode. They lead current $I+I_0$ where I is total current and I_0 is saturation current. This current generates shot noise as written in Eq. 8. 2) Electrons from p to n$^+$ region corresponding to current $-I_0$. This current also generates shot noise similarly. 3) Electrons from n$^+$ and returned to n$^+$ region before recombination by back diffusion before recombination. This diffusion is thermal process. At DC or low-frequency, the noise generated by this process is called thermal noise and $S_I = 4kTg_0$ where g_0 is DC conductance. At high-frequency, AC conductance $g(f)$ increases from DC value g_0. The difference $g(f) - g_0$ also comes from same back diffusion as thermal process. Thus this increased conductance generates excess noise $4kT(g(f) - g_0)$ likely to thermal noise. Consequently, current shot noise spectrum density $S_I(f)$ is sum of each noise caused by above components and written as

$$S_I(f) = 2q(I + 2I_0) + 4kT\left[g(f) - g_0\right]. \tag{11}$$

In this equation, the first term is frequency-independent shot noise caused by the sum of above components 1 and 2. The second term is frequency-dependent RF shot noise caused by component 3 as the enhancement of AC conductance.

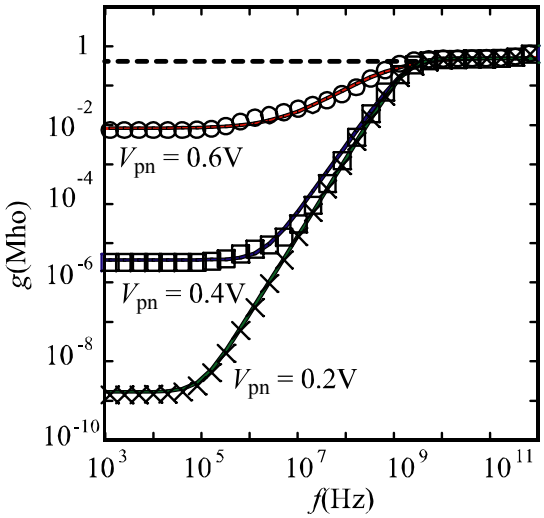

Fig. 4 AC conductance $g(f)$ of p-n diode for different V_{pn} calculated by Hara. Symbols are results of MEDICI calculations, and solid lines are the value estimated from approximation equation. Dashed line is high-frequency saturation value of $g(f)$.

In high-frequency region, Eq. 11 is dominated by AC conductance $g(f)$. Figure 4 is calculated AC conductance obtained by two different methods plotted against frequency. In this figure, symbols are AC conductance of p-n diode calculated by MEDICI and lines are the value estimated by below approximation equation. Applied forward bias V_{pn} are less than built-in potential where shot noise should be generated. At low frequency, MEDICI calculation indicates that total conductance $g(f)$ is nearly equal to g_0. In this region, conductance g_0 is mainly dominated by the conductance of diffusion layer. At higher frequency, however, $g(f)$ becomes quite higher than g_0 and saturates at ultrahigh frequency. This conductance

obtained by MEDICI calculation is approximately expressed as

$$g(f) = g_0 \frac{1+(\omega\tau_1)^{\alpha}}{1+(\omega\tau_2)^{\alpha}}, \quad (12)$$

and

$$\alpha \equiv \ln\left(\frac{g'}{g_0}\right) \Big/ \ln\left(\frac{\tau_1}{\tau_2}\right), \quad (13)$$

where g' is high-frequency saturation value of $g(f)$, τ_1 is carrier lifetime, and τ_2 represents inverse of cutoff frequency of the junction. The estimated AC conductance of p-n diode from Eqs. 12 and 13, lines in Fig. 4, well agree with measured noise spectrum as shown in section 4.

3.2 Shot Noise in MOSFET Drain Current

In the case of MOSFET, there are two p-n junctions at source-bulk and drain-bulk interfaces. Drain current I_D flows through conduction channel and these two junctions. Thus the equivalent circuit of n-MOSFET channel is as shown in Fig. 5. Here, channel region corresponds to variable resistor, which depends on channel size and is modified by V_G. At each junction, the capacitance and resistance of diffusion layer are paralleled. At DC or low-frequency region, channel resistance dominates whole conductance. However, the capacitance of each junction enhances AC conductance at RF region.

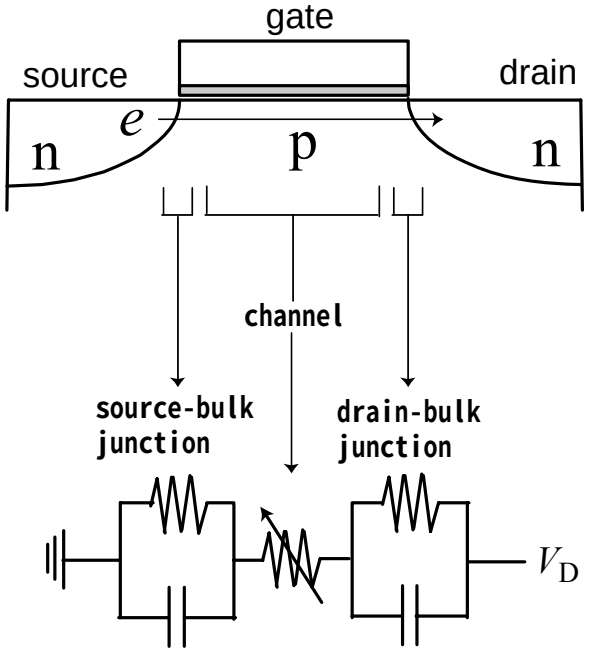

Fig. 5 Equivalent circuit of n-MOSFET channel. Each p-n junction corresponds to paralleled resistance and capacitance. Channel region corresponds to variable resistance that depends on gate voltage and channel length.

Figure 6 is surface mid-gap potential distribution of n-MOSFET between source and drain under drain voltage V_D = 1V and some gate voltage V_G calculated by MEDICI. When positive drain bias V_D is applied to n-MOSFET, electrons flow from n^+-source to p-substrate beyond junction potential barrier and then drop into n^+-drain. Therefore ONLY source-bulk junction generates junction shot noise [24-25]. As shown in the inset of Fig. 6, the height of potential barrier at source-bulk junction decreases with V_G. This result indicates that the drain current is expected to generate shot noise at sub-threshold region. In strong inversion condition, the junction potential barrier diminishes and shot noise should not be generated. If gate oxide thickness is sufficient small, gate leak current should generate gate shot noise in strong inversion [18, 22]. In this paper, we focus on drain current shot noise in sub-threshold region.

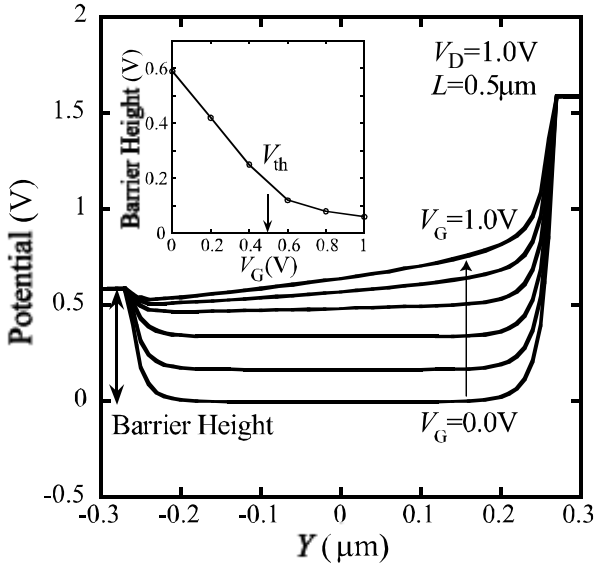

Figure 6. Calculated surface mid-gap potential distribution around MOSFET channel region for V_D = 1.0V and V_G = 0.0~1.0V. Y < -0.3μm is source region and Y > 0.3μm is drain region. The inset is V_G dependency of source-bulk junction barrier height.

At high frequency region, AC conductance of two p-n junctions (source-bulk and drain-bulk) is enhanced exponentially and dominates whole AC channel conductance $g(f)$ of MOSFET. When we assume that AC conductance of channel region is ignored, $g(f)$ is approximately expressed by AC conductance of two junctions as

$$\frac{1}{g(f)} \sim \frac{1}{g_{sb}(f)} + \frac{1}{g_{db}(f)}, \quad (14)$$

where $g_{sb}(f)$ and $g_{db}(f)$ are source-bulk and drain-bulk junction AC conductance, respectively. As discussed above, only source-bulk junction corresponds to shot noise generation and thus $g(f)$ in Eq. 11 for p-n diode is $g_{sb}(f)$ in

MOSFET. If we assume $g_{sb}(f)$ is nearly equal to $g_{db}(f)$, Eq. 14 is reduced to $g_{sb}(f) \sim 2g(f)$. Thus the shot noise model equation for MOSFET is, from Eq. 11 for p-n diode, described as

$$S_I(f) = 2q(I_D + 2I_0) + 8kT\left[g(f) - g_0\right], \quad (15)$$

where I_D is drain current, I_0 is saturation current at source-bulk junction, and g_0 is DC channel conductance dI_D/dV_D. Here g_0 can be ignored at RF region because $g(f)$ becomes quite larger.

In weak inversion, drain current I_D in MOSFET is dominated by diffusion [26]. From analogy of n-p-n bipolar transistor description, the sub-threshold drain current I_D in n-MOSFET is expressed as

$$I_D = qSD_n \frac{n_{se} - n_{de}}{L}, \quad (16)$$

where $D_n = \mu_n kT/q$ is electron diffusion coefficient, S is the cross section of current flow, and n_{se} and n_{de} are channel electron densities at source edge and drain edge, respectively. These electron densities are given by

$$n_{se} = n_{p0} e^{\beta\psi_s}, \quad (17)$$

$$n_{de} = n_{p0} e^{\beta(\psi_s - V_D)}, \quad (18)$$

where ψ_s is the surface potential at the source edge and $\beta \equiv q/kT$. Therefore, I_D is described as

$$I_D = qSD_n \frac{n_{p0} e^{\beta\psi_S}}{L}\left(1 - e^{-\beta V_D}\right). \quad (19)$$

The cross section S is calculated from channel width W and effective channel thickness kT/qE_s (E_s is the weak-inversion surface field). E_s is derived from channel charge of surface depletion region Q_B as

$$E_s = -\frac{Q_B}{\varepsilon_s} = \sqrt{\frac{2qN_A\psi_s}{\varepsilon_s}}, \quad (20)$$

where ε_s and N_A is dielectric constant and acceptor density of substrate. Thus

$$qSD_n = \frac{k^2T^2\mu_n W}{qE_s} = \frac{\mu_n W}{2\beta^2}\sqrt{\frac{2q\varepsilon_s}{N_A\psi_s}}. \quad (21)$$

From Eqs. 19 and 21, sub-threshold current is written as

$$I_D = \left(\frac{W}{L}\right)\frac{\mu_n n_{p0}}{2\beta^2}\sqrt{\frac{2q\varepsilon_s}{N_A\psi_s}}\left(1 - e^{-\beta V_D}\right)e^{\beta\psi_s}. \quad (22)$$

This current is inversely proportional to L and exponentially varies with ψ_s. Because surface potential ψ_s is modified by gate voltage V_G, I_D is exponentially depends on also V_G. On the other hand, this sub-threshold current I_D is almost independent on V_D for $V_D > 3kT/q \sim 0.1$V. From Eqs. 10 and 19, $I_D >> I_0$ when $V_D \geq 0.1$V at sub-threshold region. Therefore, we can ignore the effect of current component I_0 in our discussions. In conclusion, Eq. 15 becomes to

$$S_I(f) \sim 2qI_D + 8kTg(f). \quad (23)$$

To predict shot noise spectrum in drain current of n-MOSFET, we perform computer simulation by using MEDICI. The calculation model is as follows: channel length $L = 0.2 \sim 5.0\mu$m, channel width $W = 1.0\mu$m, donor density of source and drain region $N_D = 1.0\times10^{20}$ cm^{-3}, acceptor density of substrate $N_A = 3.0 \times 10^{17}$ cm^{-3}. Absolute temperature $T = 300$K. We calculate DC drain current I_D and small-signal AC conductance $g(f)$ for $f =$ 1kHz ~ 1THz between source and drain, and then estimate shot noise spectrum $S_I(f)$ of n-MOSFET from Eq. 23 of above model.

4. Results and Discussions

The shot noise in MOSFET drain current is quite small and difficult to observe. To confirm the validity of the above expression of shot noise, we compare results of calculation to the measurement of p-n diode current noise spectrum. In the case of p-n diode, the current noise spectrum includes observable shot noise under forward bias less than built-in potential. Figure 7 shows measured current noise spectrum of p-n diode (dotted lines) and shot noise estimated from Eqs. 11-13 and MEDICI calculation (solid lines). The reduction of measured noise amplitude around MHz is caused by high-frequency measurement limit. Therefore, the measurement and theoretical expectation for p-n diode shows good agreement at each bias condition.

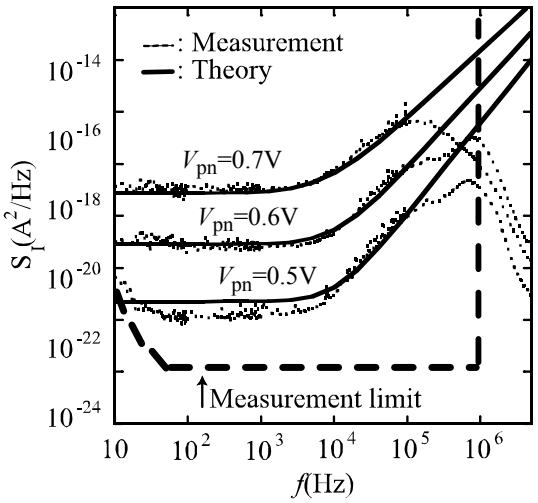

Fig. 7 Current noise spectrum density of p-n diode obtained by measurement (dotted lines) and calculation of approximation equation (solid lines) from Hara's works. Dashed line indicates measurement limit of frequency and noise intensity.

Then we shall predict shot noise in n-MOSFETs from

MEDICI calculation of drain current and small-signal AC

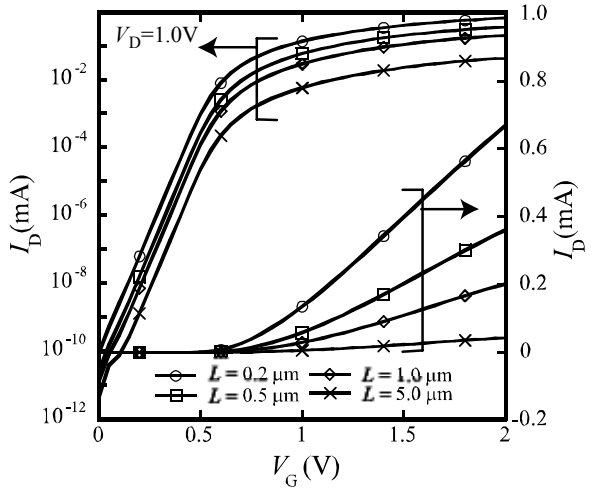

Fig. 8 I_D-V_G characteristics of n-MOSFET calculated by MEDICI for different L at V_D = 1.0V in linear and logarithmic plot.

conductance. The current-voltage characteristics of n-MOSFET model are shown in Fig. 8 (I_D-V_G plot) and Fig. 9 (I_D-V_D plot). The threshold gate voltage V_{th} is defined from Fig. 8 by using normalized drain current as $I_D L / W = 1.0 \times 10^{-7}$ A. In our calculation model, V_{th} is about 0.49V. At sub-threshold region where shot noise should be generated, Fig. 9(b) indicates that drain current reaches saturation at small V_D except for L = 0.2μm. This current I_D is used for the calculation of shot noise as the first term of Eq. 23.

Figure 10 is estimated shot noise spectrum $S_I(f)$ of n-MOSFET from MEDICI calculation for V_D = 1.0V and V_G = 0.1 ~ 0.4V at L = 0.2, 0.5, 1.0, and 5.0μm. The shot noise spectrum is made of two components: frequency-independent part caused by sub-threshold current (the first term of Eq. 23, dotted lines) and frequency-dependent part caused by back scattering of electrons (second term of Eq. 23, dashed lines). At DC or low-frequency region, the former frequency-independent part is dominant so that $S_I(f) \sim 2qI_D$. Around GHz or higher frequency region, on the other hand, the later frequency-dependent part becomes dominant and $S_I(f) \sim 8kTg(f)$.

These results indicate existence of RF shot noise independent on V_G and L. The V_G dependency of low-frequency (1kHz) and high-frequency (10GHz) shot noise at each L is shown in Fig. 11. From this figure, these two noises show apparent contrast. The low-frequency shot noise (open symbols) exponentially increases with V_G and is inversely proportional to L. In contrast, the high-frequency noise (solid symbols) is independent on L and V_G. These results can be understood as follows. At low-frequency region, shot noise is dominated by sub-threshold current I_D and thus depend on channel size and carrier density as shown in Eqs. 16 and 22. At high-

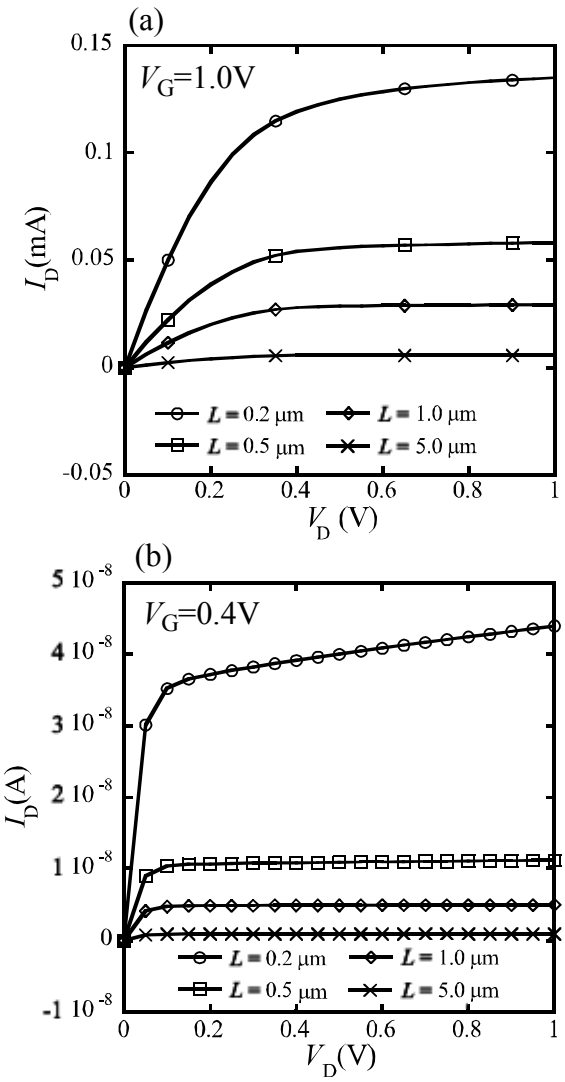

Fig. 9 I_D-V_D characteristics of n-MOSFET calculated by MEDICI for different L at (a) V_G = 1.0V in strong inversion and (b) V_G = 0.4V in weak inversion.

frequency, on the other hand, AC conductance $g(f)$ is enhanced and dominates shot noise. Here, the enhancement of $g(f)$ is caused at two p-n junctions. Therefore, RF shot noise is decided at source-bulk p-n junction and thus has no relation to channel condition such as channel length, carrier density, etc.

The V_D dependency of shot noise spectrum also indicates RF shot noise characteristics same as above discussion. Figure 12 is the effect of drain bias V_D on shot noise spectrum for V_D = 0.2 ~ 1.0V under fixed gate voltage V_G = 0.4V at each L. The V_D dependency of shot noise intensity at 1kHz (open symbols) and 10GHz (solid symbols) is shown in Fig. 13. These results are quite different from the effect of V_G as shown in Figs. 10 and 11.

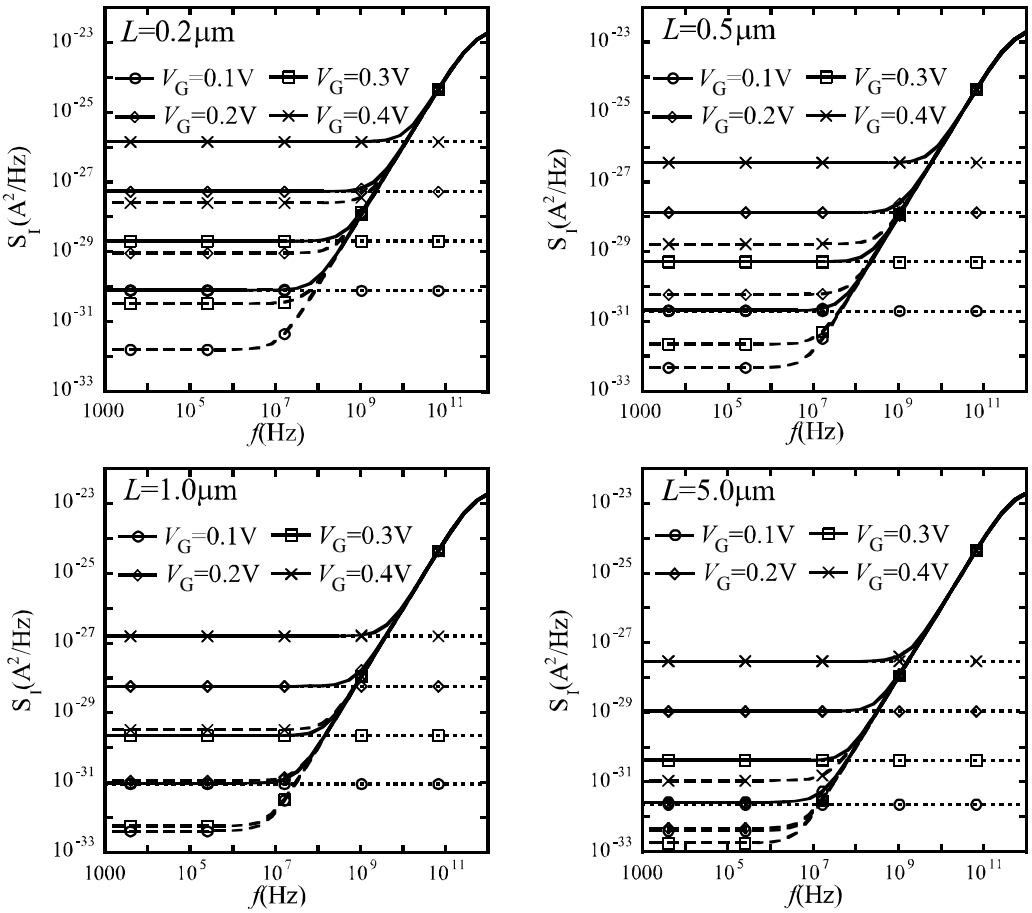

Fig. 10 V_G dependency of shot noise spectrum $S_I(f)$ for n-MOSFET at V_D = 1.0V calculated by MEDICI (solid lines), and contribution of current (dotted lines) and AC conductance (dashed lines). Low-frequency noise is dominated by sub-threshold current. High-frequency noise is dominated by AC conductance and independent on L and V_G.

At low-frequency region, shot noise is almost independent on V_D. This is easily understood that sub-threshold current I_D is almost constant for $V_D > 0.1$V as predicted by Eq. 22 or Fig. 9. On the other hand, high-frequency shot noise slightly depends on L and V_D. Here, L dependency is caused by I_D term because the difference between $2qI_D$ (dotted lines) and $8kTg(f)$ (dashed lines) is small at f = 10GHz as shown in Fig. 12. In addition, RF shot noise intensity slightly decreases with increasing V_D. This high-frequency characteristic is interpreted as bellow.

RF shot noise is defined only at p-n junctions as discussed above. Figure 14 is examples of AC conductance of p-n junction calculated by MEDICI under forward (V_{pn} = 0.4V), zero and reverse (V_{pn} = -0.4V) bias conditions. These results show that RF conductance is slightly increased by forward bias and decreased by reverse bias. When positive V_D is applied on n-MOSFET, forward bias is applied on source-bulk junction and reverse bias on drain-bulk junction. As shown in potential distribution in Fig. 5, strong electric field is applied around drain edge

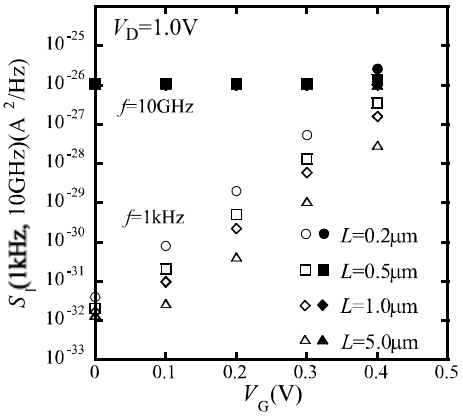

Fig. 11 Shot noise amplitude calculated from MEDICI and model equation at f = 1kHz (open symbols) and f = 10GHz (solid symbols) against V_G. At low-frequency of 1kHz, the amplitude is proportional to L^{-1} and exponentially depends on V_G. At high-frequency of 10GHz, however, noise amplitude is almost independent on above parameters.

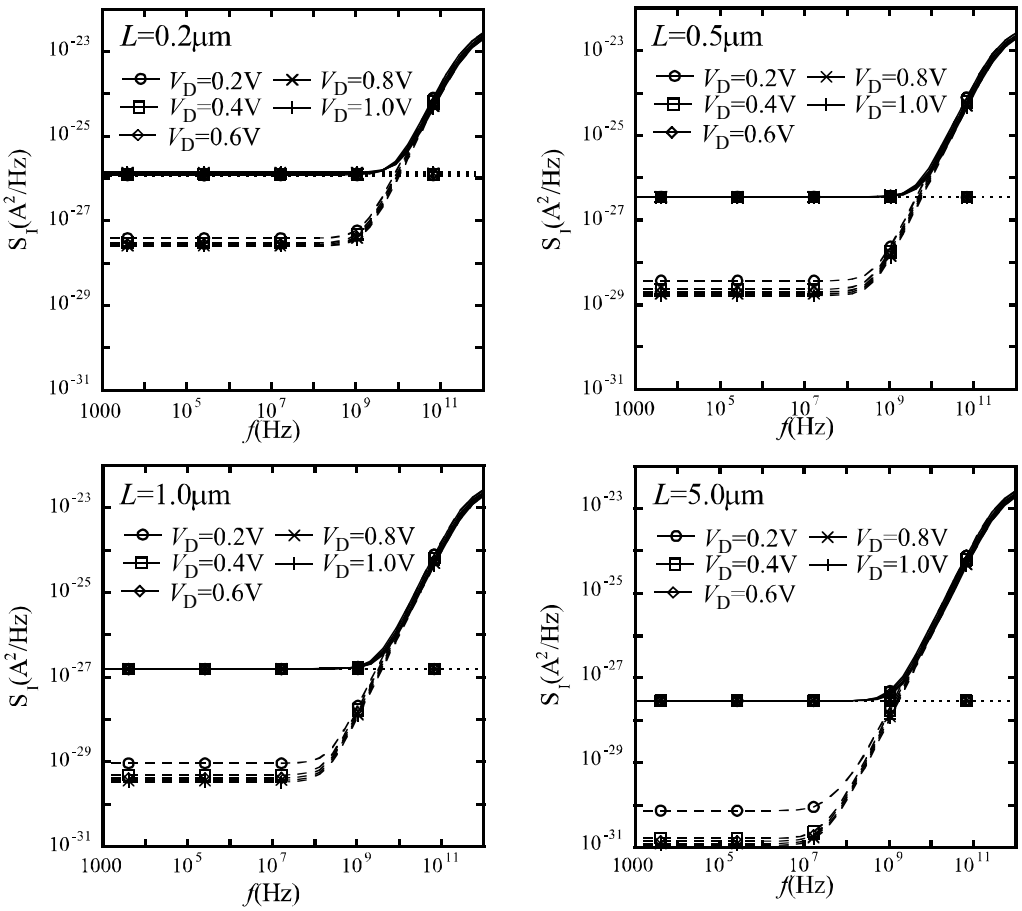

Fig. 12 V_D dependency of shot noise spectrum $S_I(f)$ for n-MOSFET at V_G = 0.4V calculated by MEDICI (solid lines), and contribution of current (dotted lines) and conductance (dashed lines). Low-frequency noise is almost independent on V_D because sub-threshold current saturates in this V_D region. High-frequency noise is independent on L and slightly decreases with V_D.

under positive V_D. Therefore, when V_D is increasing, small forward bias slightly increases at source-bulk junction and large reverse bias increases at drain-bulk junction. Thus the change of $g(f)$ - V_D characteristics of MOSFET is dominated by that of drain-bulk junction. The conductance of source-bulk junction, which generates shot noise, should be almost constant and thus actual shot noise is independent on V_D.

In conclusion these L, V_G and V_D dependency, our calculations suggest that the intensity of RF shot noise never decreases even at quite small bias condition. This means that shot noise may be serious problem at GHz or higher frequency for small-signal devices.

5. Conclusion

We have extended shot noise model for p-n diode to MOSFET. The shot noise in p-n diode is generated by conducting carrier that is crossing junction potential barrier. The predicted noise spectrum in p-n diode shows

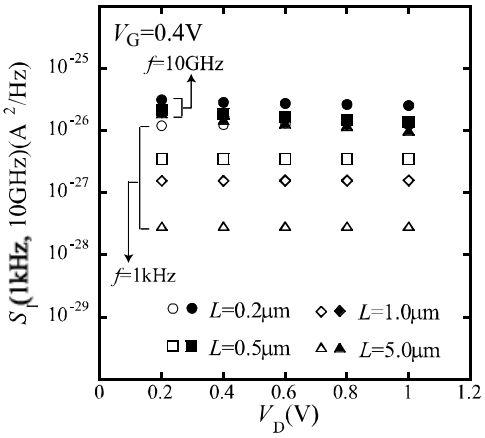

Fig. 13 Shot noise amplitude calculated from MEDICI and model equation at f = 1kHz (open symbols) and f = 10GHz (solid symbols) against V_D. At low-frequency of 1kHz, the amplitude is proportional to L^{-1} and independent on V_D. At high-frequency of 10GHz, the noise slightly decreases with increasing V_D.

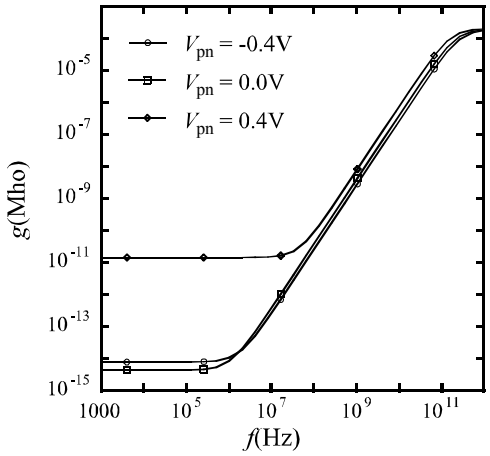

Fig. 14 AC conductance g(f) of p-n diode calculated by MEDICI under reverse (circle), zero (square), and forward (diamond) bias condition. The dopant density is same as MOSFET model. In frequency-dependent RF region, $g(f)$ slightly increases under forward bias and decreases under reverse bias.

good agreement with noise measurement. In the case of n-MOSFET, the shot noise in drain current is generated at the potential barrier of source-bulk junction. This is because conducting electrons flow from source to drain across source-bulk junction potential barrier. The height of this junction potential barrier diminishes with increasing V_G and thus shot noise should be generated in sub-threshold region. At higher V_G, not drain current but gate leak current should generate shot noise when oxide thickness is sufficiently small. We have estimated drain current shot noise spectrum in MOSFET from drain current I_D and small-signal AC channel conductance $g(f)$ calculated by MEDICI using our modeling.

Calculated shot noise spectrum is made of two components: low-frequency part of $S_I(f) \sim 2qI_D$ and high-frequency part of $S_I(f) \sim 8kTg(f)$. Low-frequency shot noise is proportional to L^{-1}, exponentially depends on V_G, but independent on V_D. High-frequency shot noise, which is dominant at GHz or higher frequency, is almost constant under various L or different bias conditions. The amplitude of RF shot noise is decided only by the conditions of source-bulk junction. This result indicates that shot noise may be serious problem at GHz or higher frequency. On small power driving of future devices, this result should be noticed.

Acknowledgments

The first author would like to thanks Professor M. Miura Mattausch, Professor T. Ezaki and the other members of the laboratory for many valuable discussions. Especially, this work is strongly based on the help of K. Hara.

References

[1] A. van der Ziel, Noise in Solid State Devices and Circuits, New York, 1986.

[2] A. van der Ziel, "Noise in Solid-State Devices and Lasers", Proc. IEEE, vol.58, no.8, pp. 1178-1205, August 1970.

[3] C. H. Chen and M. J. Deen, "High Frequency noise of MOSFETs I Modeling", Solid-State Electron., vol. 42, No. 11, pp. 2069-2081, 1998.

[4] C. H. Chen and M. J. Deen, "Channel Noise Modeling of Deep Submicron MOSFETs", IEEE Trans. Electron Devices, vol. 49, no. 8, pp. 1484-1487, August 2002.

[5] A. K. M. Ahsan and D. K. Schroder, "impact of channel carrier displacement and barrier height lowering on the low-frequency noise characteristics of surface-channel n-MOSFETs", Solid-State Electron., vol. 49, pp. 654-662, 2005.

[6] S. Asgaran, M. J. Deen, and C. H. Chen, "Analytical Modeling of MOSFETs Channel Noise and Noise Parameters", IEEE Trans. Electron Devices, vol. 51, no. 12, pp. 2109-2114, December 2004.

[7] K. Han, H. Shin, and K. Lee, "Analytical Drain Thermal Noise Current Model Valid for Deep Submicron MOSFETs", IEEE Trans. Electron Devices, vol. 51, no. 2, pp. 261-269, February 2004.

[8] S. Spedo and C. Fiegna, "Analysis of thermal noise in scaled MOS devices and RF circuits", Solid-State Electron., vol. 46, pp. 1933-1939, 2002.

[9] D. P. Triantis and A. N. Birbas, "Optimal Current for Minimum Thermal Noise Operation of Submicrometer MOS Transistors", IEEE Trans. Electron Devices, vol. 44, no. 11, pp. 1990-1995, November 1997.

[10] D. P. Triantis, A. N. Birbas, and D. Kondis, "Thermal Noise Modeling for Short-Channel MOSFET's", IEEE Trans. Electron Devices, vol. 43, no. 11, pp. 1950-1955, November 1996.

[11] E. P. Vandamme and L. K. J. Vandamme, "Critical Discussion on Unified 1/f Noise Models for MOSFETs", IEEE Trans. Electron Devices, vol. 47, no. 11, pp. 2146-2152, November 2000.

[12] L. K. J. Vandamme, "Noise as a Diagnostic Tool for Quality and Reliability of Electronic Devices", IEEE Trans. Electron Devices, vol. 41, no. 11, pp. 2176-2187, November 1994.

[13] L. K. J. Vandamme, X. Li, and D. Rigaud, "1/f Noise in MOS Devices, Mobility or Number Fluctuations?", IEEE Trans. Electron Devices, vol. 41, no. 11, pp. 1936-1945, November 1994.

[14] S. Tedja, J. van der Spiegel, and H. H. Williams, "Analytical and Experimental Studies of Thermal Noise in MOSFET's", IEEE Trans. Electron Devices, vol. 41, no. 11, pp. 2069-2075, November 1994.

[15] B. Wang, J. R. Hellums, and C. G. Sodini, "MOSFET Thermal Noise Modeling for Analog Integrated Circuits", IEEE J. Solid-State Circuits, vol. 29, no. 7, pp. 833-835, July 1994.

[16] K. K. Hung, P. K. Ko, C. Hu, and Y. C. Cheng, "A Unified Model for the Flicker Noise in Metal-Oxide-Semiconductor Field-Effect Transistors", IEEE Trans. Electron Devices, vol. 37, no. 3, pp. 654-665, March 1990.

[17] J. Lee, G. Bosman, K. R. Green, and D. Ladwig, "Noise Model of Gate-Leakage Current in Ultrathin Oxide MOSFETs", IEEE Trans. Electron Devices, vol. 50, no. 12, pp. 2499-2506, December 2003.
[18] C. Fiegna, "Analysis of Gate Shot Noise in MOSFETs With Ultrathin Gate Oxides", IEEE Electron Device Letters, vol. 24, no. 2, pp. 108-110, February 2003.
[19] A. J. Scholten, L. F. Tiemeijer, R. van Langevelde, R. J. Havens, A. T. A. Zegers-van Duijnhoven, and V. C. Venezia, "Noise Modeling for RF CMOS Circuit Simulation", IEEE Trans. Electron Devices, vol. 50, no. 3, pp. 618-632, March 2003.
[20] J. C. Ranuarez, M. J. Deen, and C. H. Chen, "Modeling the Partition of Noise From the Gate-Tunneling Current in MOSFETs", IEEE Electron Device Letters, vol. 26, no. 8, pp. 550-552, August 2005.
[21] H. F. Teng, S. L. Jang, and M. H. Juang, "A unified model for high-frequency current noise of MOSFETs", Solid-State Electron., vol. 47, pp. 2043-248, 2003.
[22] M. Koh, W. Mizubayashi, K. Iwamoto, H. Murakami, T. Ono, M. Tsuno, T. Mihara, K. Shibahara, S. Moyazaki, and M. Hirose, "Limit of Gate Oxide Thickness Scaling in MOSFETs due to Apparent Threshold Voltage Fluctuation Induced by Tunnel Leakage Current", IEEE Trans. Electron Devices, vol. 48, no. 2, pp. 259-263, February 2001.
[23] L. Pantisano and K. P. Cheung, "Origin of microwave noise from an n-channel metal-oxide-semiconductor field effect transistor", J. Appl. Phys., vol. 92, no. 11, pp. 6679-6683, December 2002.
[24] M. S. Obrecht, T. Manku, and M. I. Elmasry, "Simulation of Temperature Dependence of Microwave Noise in Metal-Oxide-Semiconductor Field-Effect Transistors", Jpn. J. Appl. Phys., vol. 39, no. 4A, pp. 1690-1693, April 2000.
[25] M. S. Obrecht, E. Abou-Allam, and T. Manku, "Diffusion Current and Its Effect on Noise in Submicron MOSFETs", IEEE Trans. Electron Devices, vol. 49, no. 3, pp. 524-526, March 2002.
[26] S. M. Sze, Physics of Semiconductor Devices, New York, 1986.

Yoshioki Isobe received the B.S. and M.S. degrees in Graduate School of Advanced Sciences of Matter, Hiroshima University in 2001 and 2003 respectively. During 2003-2004, he stayed in Department of Applied Physics, Nagoya University as Post-Doctoral Fellow. From 2004, he stayed in Research Center for Nanodevices and Systems, Hiroshima University.